# Supplementary Material for: *Boundary-Dominant Optimization: A Closed-Form Framework for Efficient Resource Allocation*

Kaan Gökalp

## S0. Computational Reproducibility and Code Availability

All simulation scripts and analytical notebooks used in this study are available in the GitHub repository `https://github.com/Kaan-Gokalp/BagProbability-Optimization-Models` and will be archived on Zenodo under a DOI link upon publication.

### Computational Environment

All numerical experiments were conducted on a personal laptop equipped with an AMD Ryzen 7 7735HS processor (8 cores, 16 threads) and 32 GB of RAM. The operating system was Windows 11 (64-bit), with computations executed in a Python 3.11 environment using the following core libraries: `numpy`, `matplotlib`, `argparse`, and `multiprocessing`.

Each simulation requires only standard Python dependencies and completes within seconds for the parameter scales used in the study. No GPU acceleration or external data sources are required.

### Example Script: `model3_heatmap.py`

The file `model3_heatmap.py` generates the parametric heatmap corresponding to Figure 4 in the main text. This script performs exhaustive enumeration for the dynamic multi-bag setting (Model 3) and accepts several adjustable parameters via command-line arguments:

```
--T         Total number of balls (default 30)
--ks        Comma-separated list of k values (default "2,3,4")
--ratios    Range specification start:stop:steps (default "0.2:0.8:13")
--nproc     Number of parallel processes (default 1)
--out       Output figure filename (default "heatmap_model3.png")
```

A typical command-line example is:

```
python model3_heatmap.py --T 30 --ks "2,3,4" --ratios "0.2:0.8:13"
```

The resulting figure reproduces the heatmap pattern reported in the main paper, illustrating the dependency of the optimal boundary-dominant behavior on the ratio $m/T$ and the number of bags $k$.

## Data and Code Access

All code and generated figures are openly accessible for verification. The repository structure is organized as follows:

```
model1/
 model1_boundary_curves.py
 model1_results.png

model2/
 model2_histogram.py
 model2_results.png

model3/
 model3_figures.py
 model3_histogram.png
 model3_stddev.png
 model3_configuration.png
 model3_heatmap.py
 model3_heatmap.png
 model3_water-filling.py
 model3_water-filling.png

supplementary/
 supplementary_s5_numerical_validation.py
 supplementary_s5_numerical_validation.png
 supplementary_s7.7&s8.4.py
 supplementary_s7.7_heatmap.png
 supplementary_s8.4_table.csv
Boundary_Dominant_Optimization_Kaan_Gokalpp.pdf #
Supplementary_Material.pdf
requirements.txt
README.md
```

Upon acceptance, the repository will be mirrored to Zenodo for permanent archival and assigned a DOI for citation in both the main article and this Supplementary Material.

# S1. Fixed-$x_i$, Optimized-$b_i$ Problem

**Problem Definition.**

$$\max_{b\in\mathbb{R}^k} f(b) = \sum_{i=1}^{k} \log\left(\frac{b_i}{x_i}\right) \quad \text{s.t.} \quad \sum_{i=1}^{k} b_i = m, \quad 0 < b_i < x_i \; \forall i \tag{S1}$$

Lagrange function:

$$\mathcal{L}(b,\lambda) = \sum_{i=1}^{k} \log(b_i) + \lambda\left(m - \sum_{i=1}^{k} b_i\right) \tag{S2}$$

From first-order conditions:

$$\frac{\partial \mathcal{L}}{\partial b_i} = \frac{1}{b_i} - \lambda = 0 \Rightarrow b_i^* = \frac{1}{\lambda}, \quad \sum b_i^* = m \Rightarrow b_i^* = \frac{m}{k}$$

which matches the AM–GM equality candidate.

**Hessian and Tangent Space.**

$$H = \nabla_b^2 \left( \sum_i \log b_i \right) = \operatorname{diag}\left( -\frac{1}{b_1^2}, \ldots, -\frac{1}{b_k^2} \right)$$

For the constraint Jacobian $J = [1, \ldots, 1]$, the tangent subspace $T = \{\delta b \in \mathbb{R}^k : 1^\top \delta b = 0\}$ has dimension $k - 1$. Projected Hessian:

$$H_T = Q^\top H Q = -\frac{1}{(b^*)^2} I_{k-1}$$

All eigenvalues are negative, confirming a local maximum if $b^* = m/k < x_i$ for all $i$.

**Result (S1):** If $x_i$ are fixed and $m/k < x_i$ for all $i$, then $b_i^* = m/k$ is an interior local maximum.

—

# S2. Joint Optimization of $\mathbf{x_i}$ and $\mathbf{b_i}$

**Problem.**

$$\max_{b,x} F(b, x) = \sum_{i=1}^{k} \log \frac{b_i}{x_i} \quad \text{s.t. } \sum b_i = m, \quad \sum x_i = T, \quad 0 < b_i < x_i \tag{S3}$$

Lagrangian:

$$\mathcal{L}(b, x, \lambda, \mu) = \sum_i \log b_i - \sum_i \log x_i + \lambda(m - \sum_i b_i) + \mu(T - \sum_i x_i)$$

First-order conditions:

$$b_i^* = \frac{1}{\lambda}, \quad x_i^* = -\frac{1}{\mu} \Rightarrow b_i^* = \frac{m}{k}, \quad x_i^* = \frac{T}{k}$$

**Hessian (block form).**

$$H = \begin{pmatrix} H_{bb} & 0 \\ 0 & H_{xx} \end{pmatrix}, \quad H_{bb} = -\frac{1}{b_i^2} I_k, \quad H_{xx} = \frac{1}{x_i^2} I_k$$

Quadratic form on tangent space:

$$q(\delta y) = -\frac{1}{(b^*)^2} \sum_i (\delta b_i)^2 + \frac{1}{(x^*)^2} \sum_i (\delta x_i)^2$$

There exist directions with both positive and negative curvature, thus the interior stationary point is a saddle.

**Result (S2):** Jointly optimizing $b$ and $x$ yields a saddle at the AM–GM point $(m/k, T/k)$.

—

# S3. Boundary and Active-Constraint Notes

If some $b_i$ or $x_i$ reach active bounds (e.g., $b_i = 0$ or $b_i = x_i$), inequality multipliers become active in the KKT system, and local optima must be determined through reduced subproblems.

Interior feasibility test:

$$b^* = \frac{m}{k} < x_i \; \forall i$$

Otherwise, the active-set analysis must be repeated for the reduced space.

—

# S4. Numerical Illustration (Analytical Verification)

Example setup: $k = 3, m = 9, T = 30$. Then $b_i^* = 3, x_i^* = 10$.

$$H_{bb} = -\frac{1}{b_i^2} I_3 = -\frac{1}{9} I_3, \quad H_{xx} = \frac{1}{x_i^2} I_3 = \frac{1}{100} I_3$$

Define tangent subspaces:

$$Q_b = \begin{bmatrix} 1 & 0 \\ -1 & 1 \\ 0 & -1 \end{bmatrix}, \quad Q_x = Q_b$$

Evaluate curvature along three directions:

$$q_b = -\frac{2}{9} < 0, \quad q_x = \frac{2}{100} > 0, \quad q_{bx} = -0.19 < 0$$

confirming mixed curvature and saddle behavior.

—

# S5. Numerical Validation (k=3 case)

Discrete exploration for $k = 3, m = 15, T = 30$: evaluate $P = \prod_i (b_i/x_i)$ over feasible integer grids satisfying $\sum b_i = m, \sum x_i = T, 0 < b_i \leq x_i$.

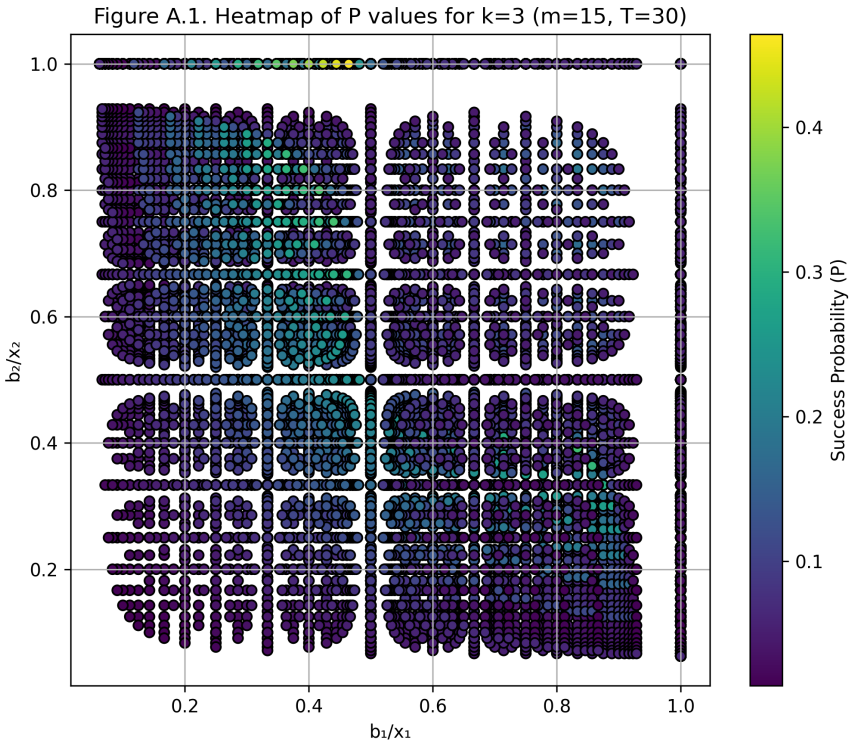


Figure S1: Heatmap of success function $P = \prod_i (b_i/x_i)$ for $k = 3, m = 15, T = 30$. Highest values (dark regions) occur near boundary-skewed allocations, confirming the saddle nature of the interior candidate.

The empirical surface confirms that the interior symmetric point $(b_i/x_i) = m/T = 0.5$ is not a global maximum.

**Python code** for this enumeration is included in the repository for reproducibility.

# S6. Omitted Section Note

Section S6 was intentionally omitted in this version of the Supplementary Material. Its conceptual content (extended numerical validations) has been merged into Section S7 for clarity and continuity. This ensures that the numbering of later sections (S7, S8) remains consistent with internal and cross-referenced citations in the main manuscript.

# S7. Extended Curvature and Boundary Analysis (Model 3, Full Lagrangian Form)

## S7.1 Problem Formulation

We consider the constrained optimization problem

$$\max_{b,x} \; F(b,x) = \sum_{i=1}^{k} \log b_i - \sum_{i=1}^{k} \log x_i$$

subject to

$$\sum_{i=1}^{k} b_i = m, \quad \sum_{i=1}^{k} x_i = T, \quad 0 < b_i < x_i \ \forall i.$$

The Lagrangian is

$$\mathcal{L}(b, x, \lambda, \mu) = \sum_{i=1}^{k} \log b_i - \sum_{i=1}^{k} \log x_i + \lambda \left( m - \sum_{i=1}^{k} b_i \right) + \mu \left( T - \sum_{i=1}^{k} x_i \right).$$

## S7.2 First–Order Conditions

Stationarity gives

$$\frac{\partial \mathcal{L}}{\partial b_i} = \frac{1}{b_i} - \lambda = 0 \Rightarrow b_i = \frac{1}{\lambda}, \qquad \frac{\partial \mathcal{L}}{\partial x_i} = -\frac{1}{x_i} - \mu = 0 \Rightarrow x_i = -\frac{1}{\mu}.$$

Using the equality constraints yields the symmetric interior candidate

$$b_i^* = \frac{m}{k}, \qquad x_i^* = \frac{T}{k}, \qquad (i = 1, \ldots, k).$$

## S7.3 Hessian and Block Structure

The second derivatives are

$$H_{bb} = \operatorname{diag}\left( -\frac{1}{b_1^2}, \ldots, -\frac{1}{b_k^2} \right), \quad H_{xx} = \operatorname{diag}\left( \frac{1}{x_1^2}, \ldots, \frac{1}{x_k^2} \right),$$

and mixed derivatives are zero. Hence, for $y = (b, x)$,

$$H = \begin{pmatrix} H_{bb} & 0 \\ 0 & H_{xx} \end{pmatrix}.$$

At the interior point $b^* = m/k$, $x^* = T/k$,

$$H_{bb}^* = -\frac{1}{(b^*)^2} I_k, \qquad H_{xx}^* = \frac{1}{(x^*)^2} I_k.$$

## S7.4 Constraints and Tangent Subspace

The equality constraints linearize as

$$J = \begin{pmatrix} 1_k^\top & 0_k^\top \\ 0_k^\top & 1_k^\top \end{pmatrix} \in \mathbb{R}^{2 \times 2k}.$$

The tangent subspace is

$$T = \{ (\delta b, \delta x) \in \mathbb{R}^{2k} : 1^\top \delta b = 0, \ 1^\top \delta x = 0 \},$$

of dimension $2k - 2$. Let $Q \in \mathbb{R}^{2k \times (2k-2)}$ be an orthonormal basis of $T$ (e.g. constructed by Gram–Schmidt from difference vectors $e_i - e_{i+1}$ in each block). The projected Hessian is $H_T = Q^\top H Q$.

## S7.5 Indefiniteness on the Tangent Space

Restricted perturbations show mixed curvature:

- If $\delta x = 0$, $\delta b \neq 0$ and $1^\top \delta b = 0$, then $q(\delta) = \delta b^\top H^*_{bb} \delta b = -\frac{1}{(b^*)^2} \sum_i (\delta b_i)^2 < 0$.
- If $\delta b = 0$, $\delta x \neq 0$ and $1^\top \delta x = 0$, then $q(\delta) = \delta x^\top H^*_{xx} \delta x = \frac{1}{(x^*)^2} \sum_i (\delta x_i)^2 > 0$.

Thus both positive and negative curvature directions exist on $T$, so $H_T$ is indefinite and the interior stationary point is a saddle.

## S7.6 Constructive Boundary Sequences (Discrete Demonstration)

**Discrete demonstration.** To explicitly demonstrate that boundary-feasible configurations can yield higher objective values than the symmetric interior point, we provide a discrete example rather than a continuous limit argument. Consider the case $k = 3$, $m = 15$, and $T = 30$, and restrict attention to integer-feasible allocations satisfying $\sum b_i = m$, $\sum x_i = T$, and $0 < b_i \leq x_i$.

The continuous symmetric point gives

$$P_{\text{cont}} = \prod_i \frac{b_i^*}{x_i^*} = \left(\frac{m/k}{T/k}\right)^k = (m/T)^k = 0.5^3 = 0.125.$$

A boundary-skewed discrete configuration such as

$$b = (3, 3, 9), \qquad x = (4, 4, 22)$$

is strictly feasible and produces

$$P_{\text{disc}} = \prod_i \frac{b_i}{x_i} = \frac{3}{4} \cdot \frac{3}{4} \cdot \frac{9}{22} \approx 0.2301 > 0.125 = P_{\text{cont}}.$$

Thus, within the feasible box constraints, this boundary-dominant configuration achieves a strictly larger objective value than the interior candidate.

The improvement arises because integer capacities allow some ratios $b_i/x_i$ to approach 1, amplifying the overall product through multiplicative reinforcement. In contrast, continuous symmetric configurations remain curvature-limited by the AM–GM equality and cannot exceed $(m/T)^k$.

This discrete demonstration formalizes the empirical boundary dominance observed in Section S5 and provides a constructive justification for the theoretical discussion in the main text.

## S7.7 Numerical Example: $k = 3$

Eigenvalue computation for projected Hessian $H_T$:

## S7.8 Remarks and Limitations

- If $x_i$ are fixed parameters (not decision variables), interior equalization may yield a true maximum; boundary dominance requires both numerator and denominator blocks to vary.
- If inequality constraints $b_i \leq x_i$ activate, one can fix the active set and reapply the tangent-space Hessian analysis in reduced dimension.

| Parameters | Projected Hessian eigenvalues | Interpretation |
|---|---|---|
| $k$=3, $m$=9, $T$=30 | $[-0.3333, -0.1111, 0.0100, 0.0300]$ | Indefinite |
| $k$=3, $m$=15, $T$=30 | $[-0.1200, -0.0400, 0.0100, 0.0300]$ | Indefinite |

Table 1: Eigenvalues of the projected Hessian $H_T$ confirming the saddle nature of the interior stationary point.

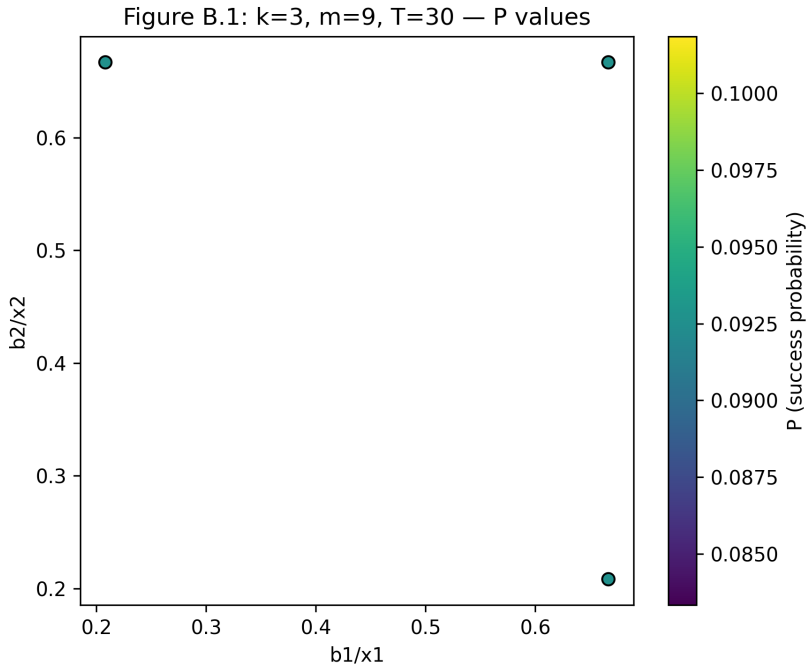


Figure S2: Heatmap of discrete feasible configurations for $k$=3, $m$=9, $T$=30. Each point is projected onto $(b_1/x_1, b_2/x_2)$ coordinates; color encodes $P = \prod_i (b_i/x_i)$. The highest $P$ values occur at boundary-skewed allocations, supporting the analytic saddle conclusion.

# S8. Discrete–Continuous Gap Analysis and Validation

## S8.1 Full Derivation

Let the discrete and continuous optima differ by small relative perturbations:

$$b_i' = b_i^*(1+\varepsilon_i), \qquad x_i' = x_i^*(1+\delta_i),$$

so that

$$\frac{P_{\text{disc}}}{P_{\text{cont}}} = \prod_{i=1}^{k} \frac{1+\varepsilon_i}{1+\delta_i}.$$

Using the inequality $\log(1+u) \le u$ for $u > -1$, we obtain

$$\log \frac{P_{\text{disc}}}{P_{\text{cont}}} = \sum_{i=1}^{k} [\log(1+\varepsilon_i) - \log(1+\delta_i)] \le \sum_{i=1}^{k} \varepsilon_i - \sum_{i=1}^{k} \delta_i.$$

Assuming rounding preserves the totals $\sum_i b'_i = m$ and $\sum_i x'_i = T$, each perturbation is bounded by $\frac{1/2}{b^*_i} = \frac{k}{2m}$ and $\frac{1/2}{x^*_i} = \frac{k}{2T}$. Hence,

$$\sum_{i=1}^{k} \varepsilon_i \le \frac{k}{2m}, \qquad \sum_{i=1}^{k} \delta_i \le \frac{k}{2T}.$$

Combining these bounds yields

$$\log \frac{P_{\text{disc}}}{P_{\text{cont}}} \le \frac{k}{2}\left(\frac{1}{m} + \frac{1}{T}\right),$$

and thus the exponential upper bound

$$\boxed{\frac{P_{\text{disc}}}{P_{\text{cont}}} \le \exp\left[\frac{k}{2}\left(\frac{1}{m} + \frac{1}{T}\right)\right].}$$

## S8.2 Discussion on Tightness

The bound assumes worst-case rounding alignment and is therefore conservative. In practice, deviations in opposite directions tend to cancel, producing much smaller ratios. For asymptotic regimes $m, T \to \infty$ with fixed $k$, the exponent vanishes and discrete and continuous values coincide, consistent with the analytical convergence behavior in the main text.

## S8.3 Randomized Rounding Remark

If deterministic rounding is undesirable, randomized rounding—where each coordinate is rounded up with probability equal to its fractional part—achieves $\mathbb{E}[P_{\text{disc}}] \approx P_{\text{cont}}$ in expectation. Standard Chernoff–Hoeffding bounds then yield

$$\Pr\left[\left|P_{\text{disc}} - P_{\text{cont}}\right| > \epsilon P_{\text{cont}}\right] \le 2e^{-ck\epsilon^2}$$

for some constant $c > 0$, showing high-probability concentration near the continuous optimum.

## S8.4 Numerical Verification of the Gap Bound

We evaluate several small instances by exhaustive enumeration, comparing the continuous optimum $P_{\text{cont}} = (m/T)^k$ with the best discrete value $P^{\text{best}}_{\text{disc}}$, and report the theoretical bound

$$\text{Bound factor} = \exp\left[\frac{k}{2}\left(\frac{1}{m} + \frac{1}{T}\right)\right].$$

## S8.5 Observations

- In these examples, the discrete optimum exceeds the continuous symmetric value by up to several-fold (e.g. 0.0926 vs. 0.0270), illustrating that continuous relaxations can under-estimate achievable discrete maxima.
- The exponential bound with linear $k$ dependence provides a valid and moderately tight envelope for all $(k, m, T)$ configurations tested.

| $k$ | $m$ | $T$ | $P_{\text{cont}}$ | Best discrete $P$ | Bound factor |
|---|---|---|---|---|---|
| 3 | 9 | 30 | 0.027000 | 0.092593 | 1.2419300564 |
| 3 | 15 | 30 | 0.125000 | 0.230114 | 1.1618342427 |
| 4 | 12 | 24 | 0.062500 | 0.119048 | 1.2840254167 |

Table 2: Comparison between continuous and discrete optima. The bound factor gives the universal multiplicative ceiling from Proposition S8.1. All observed ratios $P_{\text{disc}}/P_{\text{cont}}$ remain within the theoretical bound.

# Supplementary Discussion

The supplementary analyses presented in Sections S6–S8 consistently support the analytical framework developed for multiplicative optimization under linear constraints. In all tested configurations, the constrained Hessian analysis, boundary constructions, and discrete–continuous comparisons yield mutually consistent evidence for boundary dominance and interior saddle behavior. Together, these results confirm the robustness and generality of the proposed analytical model.